VOLUME 123, NUMBER 4
JANUARY 31, 2001

JOURNAL OF THE AMERICAN CHEMICAL SOCIETY

Structure/Energy Correlation of Bowl Depth and Inversion Barrier in Corannulene Derivatives: Combined Experimental and Quantum Mechanical Analysis

T. Jon Seiders, Kim K. Baldridge, Gunther H. Grube, and Jay S. Siegel*

Contribution from the Department of Chemistry, University of California−San Diego, La Jolla, California 92093-0358

Received June 5, 2000. Revised Manuscript Received October 6, 2000

Abstract: Synthesis of a series of corannulene derivatives with varying bowl depths has allowed for a study correlating the structure (bowl depth) and the energy of bowl inversion. Substituents placed in the *peri* positions are repulsive and flatten the bowl, thus causing a decrease in the bowl inversion barrier. Conversely, annelation across the *peri* positions causes a deepening of the bowl, thus an increase in the bowl inversion barrier. Barriers between 8.7 and 17.3 kcal/mol have been measured, and their structures have been calculated using a variety of ab initio methods. The energy profile of an individual corannulene derivative is assumed to fit a mixed quartic/quadratic function from which an empirical correlation of bowl depth and inversion barrier that follows a quartic function is derived. Structure/energy correlations of this type speak broadly of the nature of enzymatic and catalytic activation of substrates.

Introduction

In contrast to graphitic polycyclic aromatic hydrocarbons (PAHs),[1] corannulene[2] (**1**) is best described as a shallow bowl (Figure 1).[3] This curvature stems from the presence of a five-membered ring centered among six-membered rings[4] and endows **1** with dynamic behavior, bowl inversion (Figure 2), where the flat conformation is a transition state between two curved bowls. Insight into the structural changes that occur along the inversion pathway of **1** is visualized through a series of corannulene derivatives with perturbed structures. The perturbations in these derivatives are designed to simulate the distortions along a model potential energy surface and serve as "snapshots" for the inversion process. With the synthetic methods to

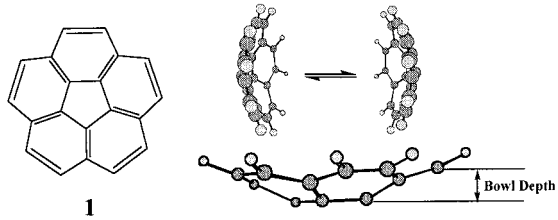

1

Figure 1. Corannulene (1) and corannulene's bowl inversion.

(1) Harvey, R. G. *Polycyclic Aromatic Hydrocarbons*; Wiley-VCH: New York, 1997.

(2) For reviews on corannulene and related structures, see: Scott, L. T.; Bronstein, H. E.; Preda, D. V.; Ansems, R. B. M.; Bratcher, M. S.; Hagen, S. *Pure Appl. Chem.* **1999**, *71*, 209−219. Mehta, G.; Rao, H. S. P. *Tetrahedron* **1998**, *54*, 13325−13370. Rabideau, P. W.; Sygula, A. *Acc. Chem. Res.* **1996**, *29*, 235−242.

(3) For crystallograghic determination, see: Hanson, J. C.; Nordman, C. E. *Acta Crystallogr. B* **1976**, *B32*, 1147. For gas-phase electron diffraction, see: Hedberg, L.; Hedberg, K.; Cheng, P.-C.; Scott, L. T. *J. Phys. Chem. A* **2000**, *104*, 7689−7694.

(4) Beck, A.; Bleicher, M. N.; Crowe, D. *Excursions into Mathematics*; Worth Publishers: New York, 1969.

(5) Seiders, T. J.; Elliott, E. L.; Grube, G. H.; Siegel, J. S. *J. Am. Chem. Soc.* **1999**, *121*, 7804−7813.

(6) Seiders, T. J.; Baldridge, K. K.; Elliott, E. L.; Grube, G. H.; Siegel, J. S. *J. Am. Chem. Soc.* **1999**, *121*, 7439−7440.

10.1021/ja0019981 CCC: $20.00
Published on Web 01/09/2001

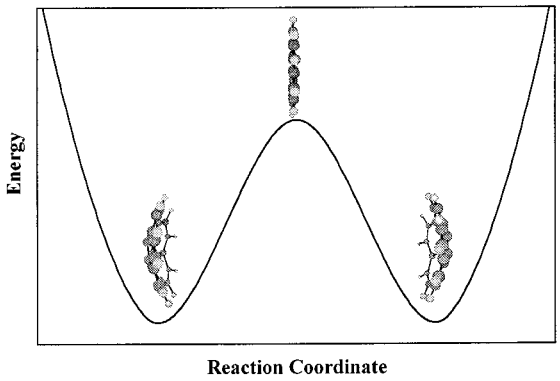

Figure 2. Energy diagram of the inversion process of 1.

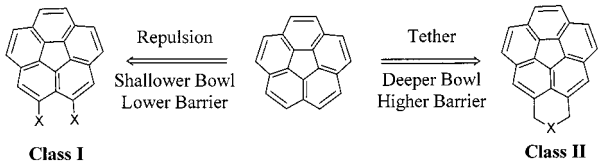

Figure 3. Target molecules for study of bowl depth/inversion barrier.

substituted corannulenes in hand,[5,6] a series of perturbed corannulene derivatives have been synthesized and a structure/energy correlation achieved.

Experimental Design

We begin from the assumption that the equilibrium bowl depth of a corannulene derivative correlates with the height of the energy barrier to bowl inversion. This assumption raises several questions. What methods will best reveal such a correlation should it exist? What molecules form an appropriate "test set" for validation of the model? What analytical function should best fit the correlation? What ramifications come from such an analysis? The question of methods can be answered fairly directly; NMR provides a large window for the measurement of dynamic processes in solution, and either high-accuracy X-ray crystallography or quantum mechanical computations provide reliable structural data. Those being the methods of choice, the commonalities among the compounds in the "test set" must be (a) synthetic accessibility, (b) structural perturbation, and (c) dynamic symmetry equivalence.

Synthetic methods to a variety of corannulene derivatives are well established.[5,6] In particular, numerous *peri* (2,3) substitutions are accessible. Interactions across the *peri* positions are envisioned to provide a wide range of bowl depths owing to either nonbonded repulsion or annelation (Figure 3). Two basic classes of *peri*-substituted corannulene derivatives arise. Derivatives in class I have bulky substituents at adjacent *peri* positions, whereas those in class II have *peri* substituents tethered together. It is presumed that bulky groups will flatten the bowl and lower the barrier, in contrast to the tethers, which will deepen the bowl and raise the barrier compared to **1**. Thus, conditions a and b are met.

The inversion process of corannulene renders the convex and concave faces equivalent and creates a dynamic mirror symmetry coincident with the time-averaged plane of the molecule. This time-averaged symmetry alters the site symmetry of a rim hydrogen from C_1 in the static molecule to C_s at the dynamic limit. Replacement of H by a $C(A_2B)$ group, for example CH_2X or $C(CH_3)_2X$, provides diastereotopic groups at the static limit, which become enantiotopic during bowl inversion. Measurements of the coalescence temperature (T_c), frequency separation ($\Delta\nu$), and geminal coupling constant (J_{gem}) allow calculation of inversion barriers, using the Gutowski−Holm approximation.[7] All compounds in the test series have such a probe; thus, condition c is met and a suitable test set of *peri* derivatives is established.

With methods chosen and compounds targeted, we come to the question of the analytical form of the correlation. We are trained to look for linear, exponential, polynomial, and related mathematical forms in a set of data, but given a model for molecular dynamics such as bowl inversion, what should be the simplest form with which to begin?

Bowl inversion relates two symmetry-equivalent minima through a common transition state. As such, the structure−energy expression should fit well to a double-well potential (Figure 2). Clearly, linear or simple quadratic behavior is not going to work. The simplest polynomial that "fits the bill" is a quartic minus a quadratic (eq 1).[8] Under this assumption, eq 1 describes the reaction profile of an individual corannulene derivative; the coefficients *a* and *b* tailor the shape of each profile. Solving for *a* and *b*, by evaluating the derivative of eq 1 (eq 2) at the extrema (eq 3), leads to the quartic relationship of inversion energy (ΔE) with equilibrium bowl depth (x_{eq}) (eq 4).

$$E = ax^4 - bx^2 \tag{1}$$

$$dE/dx = 4ax^3 - 2bx = 0 \tag{2}$$

$$x = 0 \quad b = 2a(x)^2 \tag{3}$$

$$\Delta E = E(x_{eq}) - E(x_0) = a(x_{eq})^4 - 2a(x_{eq})^2(x_{eq})^2 = -a(x_{eq})^4 \tag{4}$$

Synthesis

The corannulene derivatives of class I and II rely on a common starting material, 2,3-dichlorocorannulene (**2a**). Treatment of **2a** with trimethylaluminum in the presence of $NiCl_2$-dppp yields 2,3-dimethylcorannulene[5] (**3a**) from which photobromination with *N*-bromosuccinimide produces the bis(bromomethyl) derivative (**3b**) (Scheme 1). Treatment of **2a** with phenylmagnesium bromide in the presence of a catalytic amount of $NiCl_2$dppp[10] produced 2,3-diphenylcorannulene (**4**). The 2,3-bis(diethylene glycol methyl ether) derivative (**5**) was produced by heating **2a** in diethylene glycol monomethyl ether with an excess of sodium hydride. Independent preparation of **2d** was necessary to assess the *peri*-chloro perturbation (Scheme 2).[5,9]

A key intermediate in the synthesis of derivatives in class II is **3b**. A number of six-membered annelated derivatives have been prepared by the reaction of divalent nucleophiles with **3b** (Scheme 3). Since quantities of materials no greater than those

(7) Sandstrom, J. *Dynamic NMR Spectroscopy*; Academic Press: New York, 1982.

(8) Other symmetric double-well potentials, in particular the inversion of nitrogen, have been fit to mixed quartic/quadratic functions (eq 1); see: Dennison, D. M. *Rev. Mod. Phys.* **1940**, *12*, 175. Ha, T. K.; Dunitz, J. D. *Helv. Chim. Acta* **1990**, *73*, 583−593. In addition, a variety of out of plane ring vibrations have been fit to quartic/quadratic functions from vibrational spectra; see: Laane, J. *Int. Rev. Phys. Chem.* **1999**, *18*, 301−341.

(9) Tamao, K.; Sumitani, K.; Kumada, M. *J. Am. Chem. Soc.* **1972**, *94*, 4374−4376.

(10) Because no probe for dynamic NMR is present on **2a**, 2,7-bis(methoxymethyl)-4,5-dichlorocorannulene (**2d**) was synthesized to measure the effect of *peri*-chlorines (Scheme 1). Synthesis of **2d** starts from 2,7-dimethyl-4,5-dichlorocorannulene (**2b**), the synthesis of which parallels that of **2a**.[5] Photobromination of **2b** yields the bis(bromomethyl) derivative (**2c**). In principle, **2c** has a handle for performing the dynamic NMR study, but its solubility proved to be too poor at low temperature. Therefore, the bromides were displaced with methoxide to yield **2d**.

Scheme 1. Synthesis of Corannulene Derivatives in Class I

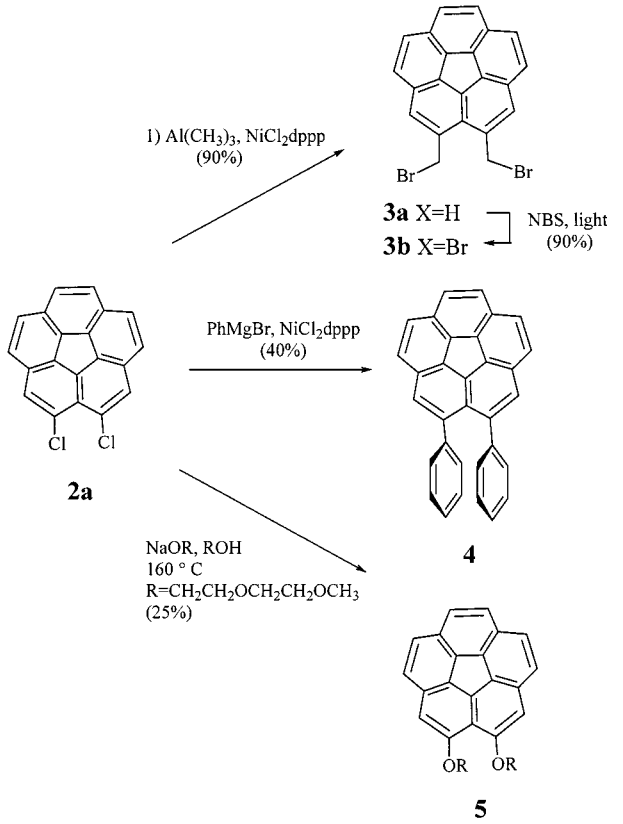

required for NMR analysis were needed, little effort was expended in optimizing the yields of these synthetic reactions. The selenide (**6**) was synthesized in one pot by reaction of 1 equiv of potassium selenocyanate with **3b** followed by in situ generation of the selenide anion with sodium borohydride and ring closure.[11] The sulfide (**7**) was synthesized by treatment of **3b** with sodium sulfide nonahydrate in dimethyl sulfoxide. The malonate derivative (**8a**) was synthesized by condensation of **3b** with diethylmalonate in an ethanolic solution of sodium ethoxide.[12] Reaction of aniline with sodium hydride and **3b** in tetrahydrofuran produced the aza derivative (**9a**). The ether derivative (**10**) was synthesized by treatment of **3b** with potassium hydroxide in 1,2-dimethoxyethane.

Acecorannulene[6,13,14] (**11**) is synthesized in low yield (20%) from **3b** by an in situ Stille type coupling using hexamethyldistannane and a palladium catalyst.[15] Alternatively, reaction of **3b** with phenyllithium produces **11** in similar yield.[16] Surprisingly, the use of low-valent titanium coupling conditions[17,18] similar to those used in the final step in the synthesis of **1**[5] yielded only trace amounts of **11** along with reduction to **3a** as the major product.

Computational Methods

Structural computations of all compounds were performed using RHF, MP2, and hybrid density functional methods (HDFT) using GAMESS[19,20] and GAUSSIAN98.[21] The HDFT method employed Becke's 3-parameter functional[22] in combination with nonlocal correlation provided by the Lee−Yang−Parr expression[23,24] that contains both local and nonlocal terms, B3LYP. Although a full suite of basis sets were investigated to establish an appropriate level, only those involving Dunning's correlation consistent basis set, cc-pVDZ,[25] a [3s2p1d] contraction of a (9s4p1d) primitive set, are reported here. These levels of theory have been previously shown to be reliable for structural determination in these types of compounds.[6,26] From the fully optimized structures, additional single point energy computations were performed using the MP2[27] dynamic correlation treatment. Chemical and physical properties such as inversion barrier, bond localization, and bowl depth are reported at RHF, B3LYP, and MP2 levels for comparison. We note a nontrivial sensitivity of predicted structure (especially bowl depth) and barrier with the inclusion of polarization functionality and with the extent and manner of including dynamic correlation. For example, in the case of **1**, dynamic correlation via HDFT predicts a barrier of 9.2 kcal/mol, whereas MP2 predicts 11.0 kcal/mol at the same basis set.[28] A more complete analysis of this effect is being investigated. Transition state analysis was done by finding the appropriate stationary points and evaluating the normal modes for a single negative eigenvalue.

Dynamics of 1 as a Parent Compound

To gauge the effect of the perturbations present in both classes of corannulene derivatives, a reference point, the inversion barrier of **1**, was established. Previously reported inversion barriers for corannulene derivatives have implicitly assumed that the probe substituent had little effect on the inversion barrier. Inversion barriers have been measured for 1-methyl-1-corannulenylethanol,[29] 2,5-bis(bromomethyl)corannulene (**12b**),[30] benzylcorannulene,[14] and isopropylcorannulene[14] with barriers of

(11) Higuchi, H.; Tani, K.; Otsubo, T.; Sakata, Y.; Misumi, S. *Bull. Chem. Soc. Jpn.* **1987**, *60*, 4027−4036.
(12) Richon, A. B.; Maragoudakis, M. E.; Wasvary, J. S. *J. Med. Chem.* **1982**, *25*, 745−747.
(13) Abdourazak, A. H.; Sygula, A.; Rabideau, P. W. *J. Am. Chem. Soc.* **1993**, *115*, 3010−3011.
(14) Sygula, A.; Abdourazak, A. H.; Rabideau, P. W. *J. Am. Chem. Soc.* **1996**, *118*, 339−343.
(15) Grigg, R.; Teasdale, A.; Sridharan, V. *Tetrahedron Lett.* **1991**, *32*, 3859−3862.
(16) Trost, B. M.; Bright, G. M.; Frihart, C.; Brittelli, D. *J. Am. Chem. Soc.* **1971**, *93*, 737−745.
(17) Olah, G. A.; Prakash, G. K. S. *Synthesis* **1976**, 607.
(18) McMurry, J. E.; Lectka, T.; Rico, J. G. *J. Org. Chem.* **1989**, *54*, 3748−3749.
(19) Schmidt, M. W.; Baldridge, K. K.; Boatz, J. A.; Jensen, J. H.; Koseki, S.; Gordon, M. S.; Nguyen, K. A.; Windus, T. L.; Elbert, S. T. *QCPE Bull.* **1990**, 10.
(20) Schmidt, M. W.; Baldridge, K. K.; Boatz, J. A.; Elbert, S. T.; Gordon, M. S.; Jensen, J. H.; Koseki, S.; Matsunaga, N.; Nguyen, K. A.; S., S.; Windus, T. L.; Dupuis, M.; Montgomery, J. A. *J. Comput. Chem.* **1993**, *14*, 1347−1363.
(21) Frisch, M. J.; Trucks, G. W.; Schlegel, H. B.; Gill, P. M. W.; Johnson, B. G.; Robb, M. A.; Cheeseman, J. R.; Keith, T. A.; Petersson, G. A.; Montgomery, J. A.; Raghavachari, K.; Al-Laham, M. A.; Zakrzewski, V. G.; Ortiz, J. V.; Foresman, J. B.; Cioslowski, J.; Stefanov, B. B.; Nanayakkara, A.; Challacombe, M.; Peng, C. Y.; Ayala, P. Y.; Chen, W.; Wong, M. W.; Andres, J. L.; Replogle, E. S.; Gomperts, R.; Martin, R. L.; Fox, D. J.; Binkley, J. S.; DeFrees, D. J.; Baker, J.; Stewart, J. P.; Head-Gordon, M.; Gonzalez, C.; Pople, J. A. *GAUSSIAN98-DFT*, Rev. A.7; Gaussian: Pittsburgh, PA, 1998.
(22) Becke, A. D. *J. Chem. Phys.* **1993**, *98*, 5648−5652.
(23) Lee, C.; Yang, W.; Parr, R. G. *Phys. Rev. B* **1988**, *37*, 785.
(24) Miehlich, B.; Savin, A.; Stoll, H.; Preuss, H. *Chem. Phys. Lett* **1989**, *157*, 200.
(25) Dunning, T. H. *J. Chem. Phys.* **1989**, *90*, 1007.
(26) Martin, J. M. L. *Chem. Phys. Lett.* **1996**, *262*, 97−104.
(27) Møller, C.; Plesset, M. S. *Phys. Rev.* **1934**, *46*, 618−622.
(28) Biedermann, P. B.; Pogodin, S.; Agranat, I. *J. Org. Chem.* **1999**, *64*, 3655−3662. For previous calculation of **1,** see references therein. For the effect of heteroatom substitution in the corannulene nucleus on bowl depth and barrier, see: Sastry, G. N.; Prakash Rao, H. S.; Bednarek, P.; Priyakumar, U. D. *Chem. Commun.* **2000**, 843−844.
(29) Scott, L. T.; Hashemi, M. M.; Bratcher, M. S. *J. Am. Chem. Soc.* **1992**, *114*, 1920−1921.
(30) Seiders, T. J.; Baldridge, K. K.; Siegel, J. S. *J. Am. Chem. Soc.* **1996**, *118*, 2754−2755.

Scheme 2. Synthesis of 2,7-Bis(methoxymethyl)-4,5-dichlorocorannulene (**2d**)

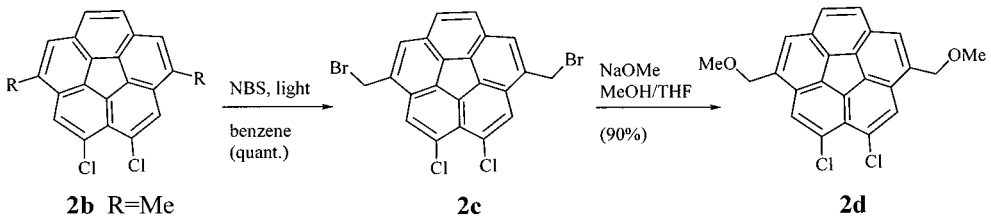

2b R=Me **2c** **2d**

Scheme 3. Syntheses of Annelated Corannulene Derivatives of Class II

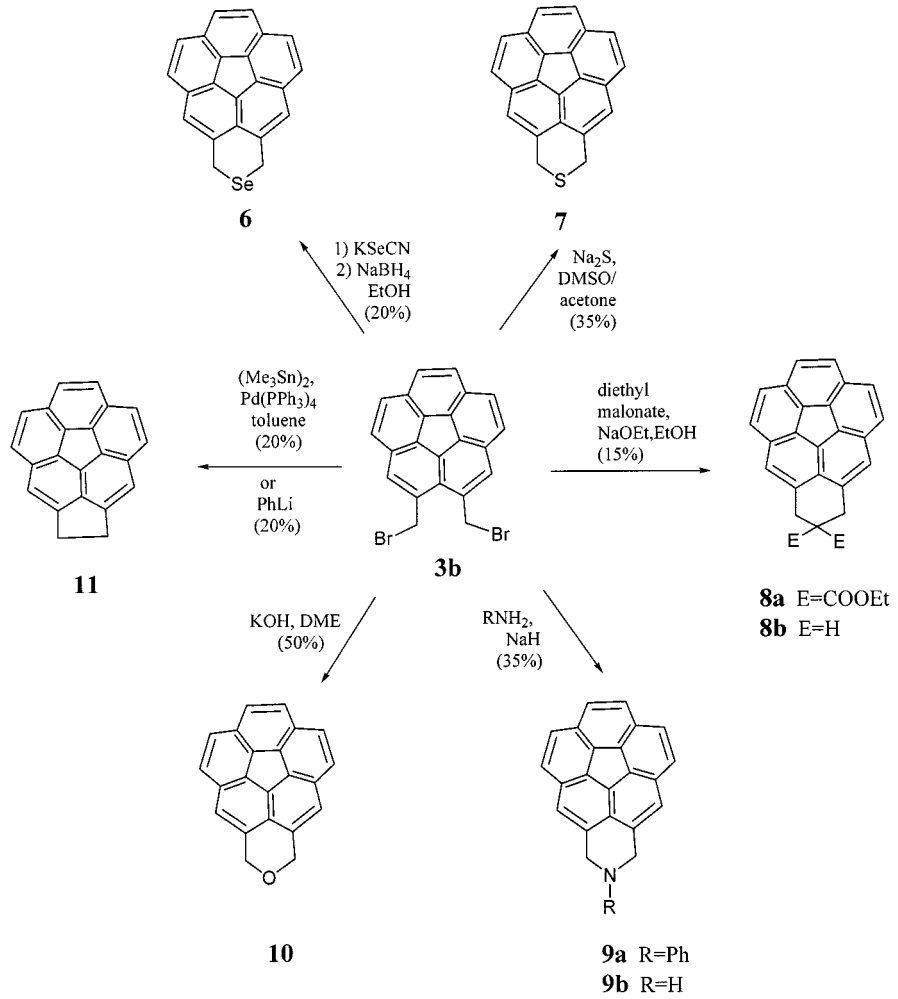

6 **7** **11** **3b** **8a** E=COOEt **8b** E=H **10** **9a** R=Ph **9b** R=H

Scheme 4. Estimation of the Inversion Barrier of Unsubstituted Corannulene

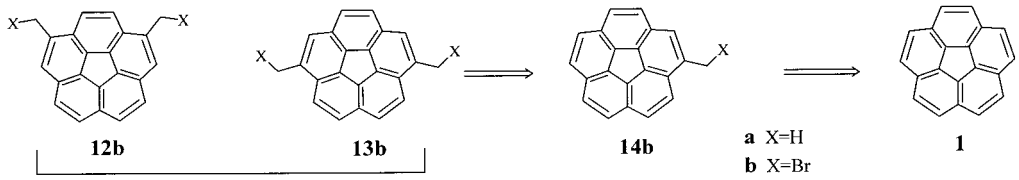

12b **13b** **14b** **a** X=H **b** X=Br **1**

10.4 - 10.5 kcal/mol **11.0 kcal/mol** **11.5 kcal/mol (estimate)**

10.2, 10.5, 11.2, and 11.3 kcal/mol respectively, but little has been done experimentally to estimate the inversion barrier of nascent corannulene. The barrier of nascent corannulene can be extrapolated from the barriers of two bis(bromomethyl)-corannulenes (**12b** and **13b**) and mono(bromomethyl)corannulene (**14b**) (Scheme 4). The barrier in **14b**, with one bromomethyl group, is 0.5 kcal/mol higher than that in either **12b** or **13b**, each with two bromomethyl groups (11.0 kcal/mol vs 10.4 or 10.5 kcal/mol, respectively). Assuming the effects of the probes are independent for **12b** and **13b**, the barrier of unsubstituted corannulene is estimated at 11.5 kcal/mol.

The dynamic bowl inversion is monitored by variable-temperature ^{1}H NMR following the diastereotopic methylene protons (compounds **2**−**14**) or *ortho* protons (in the case of **4**). Using the Gutowski−Holm approximation, the free energies of activation for the inversion processes are calculated (Table 1).[7]

Table 1. Experimental Inversion Barriers for Corannulene Derivatives

class	compd	barrier (kcal/mol)	coalescence temp (K)	$\Delta\nu$ **(Hz)**	J_{AB} (Hz)
I	**2d**[a]	8.7	180.5	41.0	10.0
	3b[b]	9.1	193.0	82.5	10.5
	4[a]	9.4	208.0	290.5	0.0
	5[a]	9.9	210.0	91.5	12.0
	12b[c]	10.4	210.5	25.5	10.0
	13b[a]	10.5	215.5	38.0	10.0
	14b[a]	11.0	223.0	24.5	10.5
parent	**1** (est.)	11.5			
II	**6**[d]	13.0	295.5	619.0	13.5
	7[d]	13.9	313.0	536.5	14.5
	8a[d]	15.5	333.0	206.0	14.5
	9a[d]	16.7	363.0	300.0	16.0
	10[d]	17.3	378.0	349.0	15.0
	11[d]	27.7	N/A	N/A	N/A

[a] CD_2Cl_2 solvent. [b] $CDCl_2F$[31] solvent. [c] THF-d_8 solvent. [d] $CDCl_2CDCl_2$ solvent.

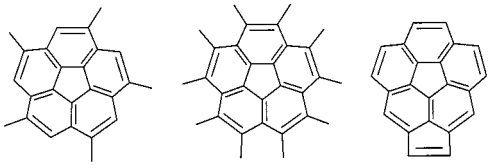

15 **16** **17**

Figure 4. Corannulene derivatives **15**−**17**.

Previously, the barrier of **11** was measured by selective deuteration of one face of the alkene precursor and monitoring the exchange by ^{1}H NMR ($\Delta G^{\ddagger} = 27.7$ kcal/mol).[14]

A cursory look at the data reveals that all class I compounds exhibit lower inversion barriers and all class II compounds exhibit higher inversion barriers than the reference inversion barrier of **1**. For class I, as the hydrogens in the 2,3 positions are replaced by larger groups, like oxygen (**5**), phenyl (**4**), bromomethyl (**3b**), or chlorine (**2a**),[32] the repulsion energyincreases between the *peri* substituents and the inversion barrier decreases relative to **1**. Conversely, for class II, as the bridging group changes from selenium (**6**) to oxygen (**10**), the methylene carbon−heteroatom bond length shortens, the methylene−methylene distance shortens and the inversion barrier increases relative to **1**. The methylene−methylene distance becomes significantly shorter upon contraction from a six-membered ring to the five-membered ring in the case of **11**, and a commensurate increase in the inversion barrier is observed. This dichotomy prompts the idea that a quantitative correlation between bowl depth and inversion barrier should exist.

Structure and Energy Parameters

High-level ab initio computations (RHF/cc-pVDZ, B3LYP/cc-pVDZ, MP2/cc-pVDZ//B3LYP/cc-pVDZ) were carried out on a series of corannulene derivatives akin to the derivatives measured experimentally (Table 2). To minimize computational time, the corannulene derivatives were abridged by substitution of hydrogen atoms in place of the carboxyethyl groups in **8a** to generate **8b** and the bromine atoms in **3b**, **12b**, **13b**, and **14b** to generate their hydrocarbon parents (**3a**, **12a**, **13a**, and **14a**), respectively. In addition, *sym*-pentamethylcorannulene (**15**),[6]

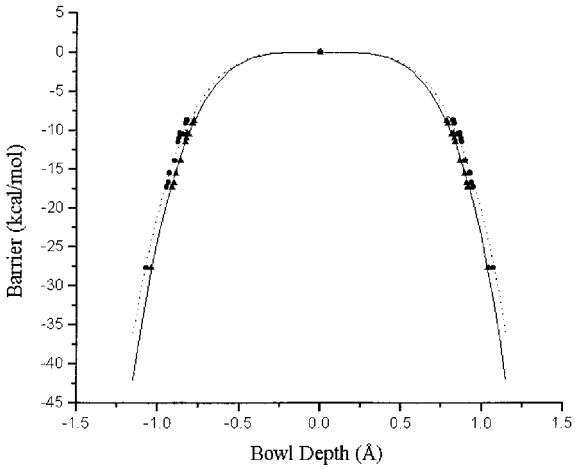

Figure 5. Structure−energy correlation of experimental inversion barrier versus calculated bowl depth of closest relative.

decamethylcorannulene (**16**),[6] and acecorannulylene (**17**)[5] (Figure 4) have been investigated computationally. The ground-state energies were compared to the transition state energies in order to deduce ΔE for bowl inversion. Transition state analysis was done by finding the appropriate stationary points and evaluating the normal modes for a single negative eigenvalue. In the case of compounds of class II, the six-member ring is puckered in the transition state to bowl inversion. Thus six-member ring inversion and bowl inversion are seen as independent processes with the former being much lower in energy that the latter. Additionally, **9b** also had a nontrivial nitrogen inversion. The three processes, bowl, ring, and atom inversion are all independent. Working through to find the appropriate stationary points is crucial to any meaningful correlation of the structure and dynamics of these compounds.

Structure Energy Correlation

As Bürgi and Dunitz have elegantly shown crystallographically, structure−energy correlations can elucidate reaction mechanisms.[33,34] In a related ring inversion study, Bürgi has fit a ring inversion barrier versus the distortion from planarity of a series of metallacyclopentenes to a similar quartic function.[35] The conclusion made from the study of metallacyclopentenes suggests "the empirical correlation between ground state structure and activation barrier is directly related to a model potential describing the energy profile of a given molecule along its way to the transition state."

To obtain a structure−energy correlation for corannulene derivatives, the inversion barriers are plotted against the bowl depths and normalized to a common transition state energy (Figures 5 and 6). Gratifyingly, our fundamental assumption of a quartic dependence between structure, equilibrium bowl depths (x_{eq}), and energy inversion barriers ($\Delta G^{\ddagger}$) leads to a beautiful fit of the data via eq 4. This realization identifies *a* as a constant among derivatives in the test set of compounds and *b* as the variable which accounts for the particular shape of the double-well potential in a given derivative.

Correlation between either the experimentally determined or the computationally derived inversion barrier and the calculated bowl depth fit well to a quartic function. Experimental structural data are available for corannulene (bowl depth = 0.87 Å).

(31) Siegel, J. S.; Anet, F. A. L. *J. Org. Chem.* **1988**, *53*, 2629−2630.
(32) Assuming the effects of the methoxymethyl groups of **2d** are similar to those of the bromomethyl groups of **12b** (∼0.5 kcal/mol decrease in barrier per bromomethyl group), an estimate of 9.7 kcal/mol for the inversion barrier of **2a** can be derived by subtracting the effect of the methoxymethyl substituents in **2d**.
(33) Bürgi, H. B.; Dunitz, J. D. *Structure Correlation*; VCH: Weinheim, New York, 1994.
(34) Bürgi, H. B. *Acta Crystallogr.* **1998**, *A54*, 873−885.
(35) Bürgi, H. B.; Dubler-Steudle, K. C. *J. Am. Chem. Soc.* **1988**, *110*, 4953−4957.

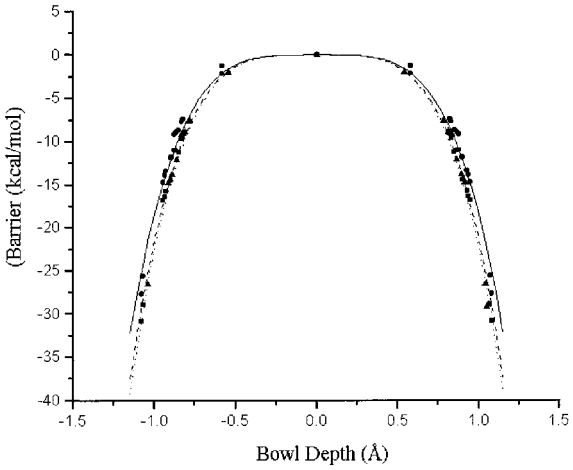

Figure 6. Structure−energy correlation of calculated inversion barrier versus calculated bowl depth.

B3LYP/cc-pVDZ best reproduces this crystallographically determined bowl depth, whereas MP2/cc-pVDZ//B3LYP/cc-pVDZ reproduces the experimentally determined inversion barriers the closest.

The correlation between activation energy and bowl depth can be thought of as a perturbation of a reference molecule, in this case 1. Two types of perturbations, repulsive or attractive interactions across the *peri* positions, govern the structure of the corannulene nucleus. Repulsive interactions, either electrostatic or steric in origin, cause a flattening of the bowl and a decrease in the inversion activation energy. Attractive interactions, either a bond or a pinching together (via cyclization), cause a deepening of the bowl and an increase in the activation energy.

The correlation obtained suggests that at relatively deep bowl depths, >0.7 Å, small changes in structure correspond to large changes in energy. Conversely, at relatively shallow bowl depths, <0.7 Å, large changes in structure correspond to small changes in energy. A particularly striking example is the bowl depth and inversion barrier for **16**. Whereas the bowl depth for **16** is calculated to be 0.582 Å, roughly 2/3 the depth of **1**, the barrier has dropped to a mere 1.3 kcal/mol (ca. 10% of that for **1**). A barrier of 1.3 kcal/mol, which is over 1 kcal/mol less than the barrier to rotation around the carbon−carbon bond of ethane, corresponds to a rate of roughly 10^{11} inversions per second at room temperature! Such a large structural change from ground state to transition state with a barrier of only 1.3 kcal/mol is a quite astonishing example of large-amplitude low-energy dynamics.

The gradual change in reaction profile for the series of corannulene derivatives can be viewed as the addition of a structural perturbation that changes the reaction profile of nascent corannulene, $E = ax^4 - bx^2$ (Figure 7). Whereas a remains constant, b varies depending on the amount of perturbation, and thus, b defines the shape of the potential (Figure 8). When b is large, as in the case of acecorannulene (**11**), the contribution from the bx^2 term is large and the double-well potential is relatively deep. When b is small, in the case of decamethylcorannulene (**16**), the contribution of the bx^2 term is small and the double well is relatively shallow. When b changes sign from positive to negative, the equation describing the energy profile becomes continuously positive (i.e., the potential is converted into a single well). A single-well potential for a corannulene derivative is satisfied when the ground-state destabilizations overcome the inherent inversion barrier of corannulene. When b is very small, the shape of the potential resembles ax^4. When b is negative and large, the shape of the potential resembles bx^2. For either single-well scenarios, at small structural changes typical of those observed in molecular vibrations, the potential is similar to that observed for the symmetric out of plane vibrations of flat aromatic hydrocarbons such as benzene.[36] This work, previous computational studies,[37,38] and the literature rich with examples of nonplanar aromatic compounds,[39] dispel the notion that aromatic compounds are confined to flat or rigid structures!

Conclusions

Investigation of corannulene derivatives with varying bowl depths has allowed for a study relating the structure and the energy of bowl inversion. Repulsive *peri* interactions flatten the bowl and cause a decrease in the bowl inversion barrier. Attractive *peri* interactions deepen the bowl and cause an increase in the bowl inversion barrier. The energy profile of an individual corannulene derivative is identified to fit a mixed quartic/quadratic function and leads to an empirical correlation of bowl depth and inversion barrier that follows a quartic function.

The observed differences in activation energy of the corannulene derivatives studied may be attributed to ground-state perturbations. Either destabilization of bowl-shaped structure, through repulsive interactions, or stabilization of the bowl-shaped structure, through attractive interactions, is the cause of the variation in activation energy rather than a transition state effect. Thus, by normalization of the energies to a common transition state level (that of the reference compound **1**), the perturbations can be viewed as a systematic alteration of the ground-state energy. Therefore, ground-state destabilization, not transition state stabilization, is at the heart of dynamic rate acceleration.

In a broader context, this structure−energy correlation speaks beyond a simple explanation for the changes of dynamics in corannulene derivatives. This correlation comments on the nature of enzymatic and catalytic activation, in general. Common belief focuses on enzymes as selective binders of the transition state;[40] in contrast, the results of such structure−energy relationships suggest that enzymes may be viewed as pushing the ground-state structure of a substrate along the reaction pathway toward a common transition state.[41−43] These perturbations would effectively raise the energy of the ground state, at the expense of the binding energy to the enzyme or catalyst, and lead to enhanced rates of reaction. An additional important observation is that the quartic dependence of energy on structure should be broadly applicable,[35,44] and as such, relatively small structural changes of the ground state can translate into pronounced changes in rates of reaction.

Experimental Section

General Data. ^{1}H and ^{13}C NMR spectra were recorded on Varian (Mercury 300 MHz/400 MHz; Unity 500 MHz) or General Electric (QE 300 MHz) spectrometers with tetramethylsilane as the internal

(36) Miller, F. A.; Crawford, B. L. J. *J. Chem. Phys.* **1946**, *14*, 282−292.
(37) Lipkowitz, K. B.; Peterson, M. A. *J. Comput. Chem.* **1993**, *14*, 121−125.
(38) Wynberg, H.; Niewpoort, W. C.; Jonkman, H. T. *Tetrahedron Lett.* **1973**, *46*, 4623−4628.
(39) Sritana-Anant, Y.; Seiders, T.; Siegel, J. *Top. Curr. Chem.* **1998**, *196*, 1−43.
(40) Stryer, L. *Biochemistry*, 4th ed.; W. H. Freeman: New York, 1995.
(41) Jenks, W. P. *Catalysis in Chemistry and Enzymology*; McGraw-Hill Book Co.: New York, 1969.
(42) Jencks, W. P. *Chem. Rev.* **1972**, *72*, 706−718.
(43) Cannon, W.; Singleton, S.; Benkovic, S. *Nat. Struct. Biol.* **1996**, *3*, 821−833.
(44) Bürgi, H. B.; Dubler-Steudle, K. C. *J. Am. Chem. Soc.* **1988**, *110*, 7291−7299.

Table 2. Structure and Energy Parameters for Corannulene Derivatives

	expt	MP2/cc-pVDZ (sp)	RHF/cc-pVD Z		B3LYP/cc-pVD Z	
compd	ΔG (kcal/mol)	ΔG (kcal/mol)	ΔG (kcal/mol)	bowl depth (Å)	ΔG (kcal/mol)	bowl depth (Å)
16		1.3	2.0	0.543	2.2	0.582
2d	8.7					
2a		9.1	7.5	0.782	7.4	0.822
3b	9.1					
3a		9.6	7.7	0.789	7.7	0.830
4	9.4					
5	9.9					
12b	10.4					
12a		11.1	9.1	0.825	9.0	0.866
13b	10.5					
13a		11.1	9.1	0.825	9.0	0.865
15		11.3	8.9	0.810	8.7	0.8497
14b	11.0					
14a		11.0	9.1	0.829	9.1	0.871
1	11.5[a]	11.0	9.2	0.834 (0.87[b])	9.2	0.877
6	13.0					
7	13.9	14.5	12.1	0.863	11.8	0.898
8a	15.5					
8b		15.7	13.8	0.890	13.4	0.928
9a	16.7					
9b	16.1[c]	16.4	14.3	0.903	13.9	0.935
10	17.3	16.9	14.8	0.914	14.7	0.947
11	27.7	28.9	26.6	1.04	25.6	1.07
17		30.9	29.2	1.05	27.7	1.08

[a] Experimental estimate. [b] Experimental value. [c] Ralph Steffens personal communication.

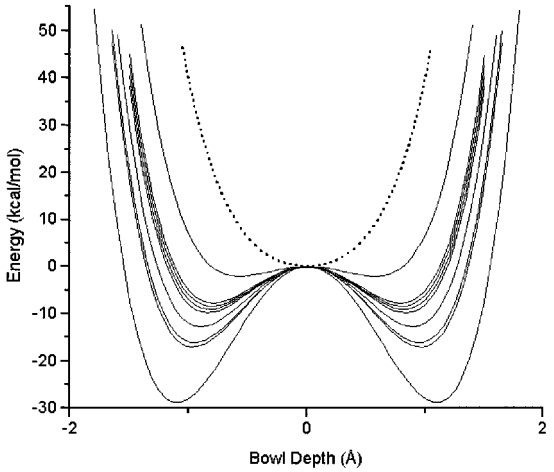

Figure 7. Reaction profiles representing the perturbation of bowl-shaped corannulene derivatives (solid lines, double-well potentials) toward flat corannulene derivatives (dashed lines, single-well potential).

standard. Low-resolution mass spectral analyses were performed in the EI-mode on a HP GC/MS 59970 spectrometer. High-resolution mass spectra were obtained from the University of California Riverside mass spectrometry facility in the FAB or DEI mode. UV/vis spectra were recorded on a Perkin-Elmer Lambda 6 UV/vis spectrophotometer. Melting points were obtained on a Mel-Temp melting point apparatus and are reported uncorrected.

Techniques and Materials. All experiments were carried out under argon in freshly distilled solvents under anhydrous conditions unless otherwise noted. Commercial chemicals were used as supplied. Tetrahydrofuran (THF), toluene, and 1,2-dimethoxyethane (DME) were distilled from sodium/benzophenone, dichloromethane was distilled from calcium hydride, and carbon tetrachloride was distilled from phosphorus pentoxide. Yields refer to chromatographically and spectroscopically (^{1}H NMR) homogeneous materials, unless otherwise stated. Characterization of all new compounds (single spot TLC) was done by melting point and ^{1}H and ^{13}C NMR, as well as by mass spectroscopy. Preparative column chromatography was performed with silica gel (230−425 mesh) from Fisher Scientific Co. Thin-layer chromatography (TLC) was performed on aluminum-backed silica gel 60 F_{254} plates from Alltech. "Centrifugal chromatography" was performed on a Chromatotron apparatus.

Experimental Methods

2,3-Bis(bromomethyl)corannulene (3b). To a 50 mL round-bottom flask equipped with a reflux condenser were added 2,3-dimethylcorannulene (**3a**) (0.320 g, 1.15 mmol) and carbon tetrachloride (30 mL) under a stream of argon. *N*-Bromosuccinimide (0.420 g, 2.36 mmol) was added to the solution followed by benzoyl peroxide (∼5 mg). The solution was irradiated with incandescent light for 4 h at room temperature. The reaction was quenched with water and extracted 3 times with water (100 mL). The organic layer was dried with magnesium sulfate, filtered, and evaporated. The solid was triturated twice with methanol (10 mL) to yield 0.450 g (90%) of a pale yellow solid. Mp: 164−166 (dec). ^{1}H NMR (500 MHz, $CDCl_3$): δ 5.40 (s, 4H), 7.78 (d, J = 9 Hz, 2H), 7.82 (s, 2H), 7.83 (d, J = 9 Hz, 2H), 7.94 (s, 2H). ^{13}C NMR (125 MHz, $CDCl_3$): δ 35.6, 126.2, 126.6, 127.7, 127.9, 129.9, 131.25, 131.28, 135.5, 135.6, 135.8, 136.4. HRMS: found, 433.9314; calcd ($C_{22}H_{12}Br_2$), 433.9306.

Acecorannulene (11). Method a. To a 250 mL round-bottom flask, toluene (125 mL) was added and degassed by bubbling with argon for 20 min. 2,3-Bis(bromomethyl)corannulene (**3b**) (0.392 g, 0.90 mmol), palladium acetate (0.020 g, 0.090 mmol), and triphenylphosphine (0.047 g, 0.178 mmol) were added at once followed by the addition of hexamethyldistannane (0.352, 1.08 mmol) by syringe. The solution was heated to reflux for 18 h and then cooled to ambient temperature. The solution was passed through a plug of silica gel and the solvent evaporated. The product was purified by centrifugal chromatography on silica gel with 10:1 hexanes to methylene chloride as the eluent to yield 0.053 (20%) g of a pale yellow solid.

Method b. Alternatively, to a 100 mL round-bottom flask 2,3-bis-(bromomethyl)corannulene (**3b**) (0.060 g, 0.22 mmol) and 50 mL of diethyl ether were added. Phenyllithium (0.44 mmol, 1.8 M in hexanes) was added over 30 min, and the solution was stirred at ambient temperature for 12 h. The reaction was quenched by slow addition of water and the organic layer washed three times with water. The organic layer was dried over magnesium sulfate, filtered, and evaporated. The crude material was purified by flash chromatography on silica gel with hexane as the eluent to yield 8 mg (20%) of a pale yellow solid. Mp: 158−160 °C. ^{1}H NMR (500 MHz, $CDCl_3$): δ 2.98 (d, J = 13 Hz,

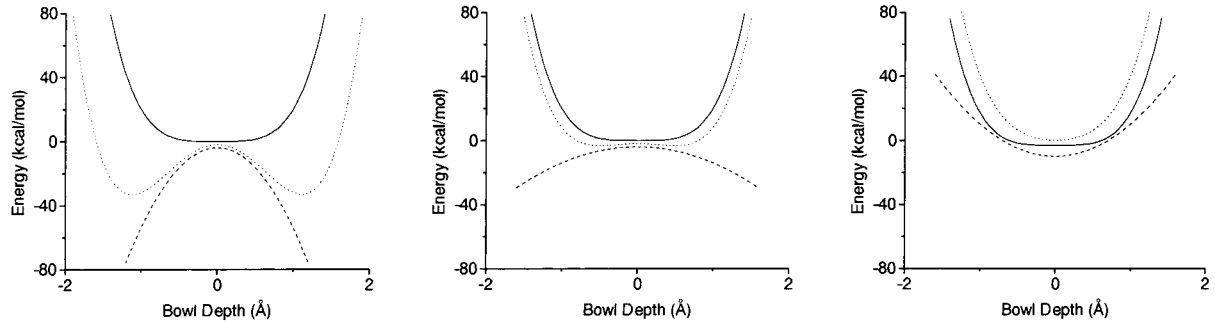

Figure 8. Addition of ax^4 and bx^2 functions. Left: $y = 20x^4 - 50x^2$. Middle: $y = 20x^4 - 20x^2$. Right: $y = 20x^4 + 20x^2$. Solid line: ax^4. Dashed line: bx^2. Dotted line: $ax^4 - bx^2$.

2H), 3.79 (d, J = 13 Hz, 2H), 7.35 (s, 2H), 7.71 (s, 4H), 7.73 (s, 2H). ^{13}C NMR (125 MHz, $CDCl_3$): δ 31.7, 121.8, 126.4, 127.0, 127.7, 130.3, 137.2, 137.6, 138.7, 139.4, 145.1, 147.7. HRMS: found, 276.0946; calcd ($C_{22}H_{12}$), 276.0939.

2,3-Dihydro-1*H*-corannuleno[2,3-*cd*]selenopyran (6). To a 50 mL round-bottom flask equipped with a reflux condenser were added 2,3-bis(bromomethyl)corannulene (**3b**) (0.050 g, 0.115 mmol), potassium selenocyanate (0.017 g, 0.115 mmol), and ethanol (25 mL) under a stream of argon. The reaction was heated to reflux for 20 min. The solution was cooled to room temperature, sodium borohydride (0.013 g, 0.344 mmol) was added, and the solution was reheated to reflux for an additional 20 min. The reaction was cooled to ambient temperature, quenched with water, diluted with methylene chloride (25 mL), and extracted three times with water (100 mL). The organic layer was dried with magnesium sulfate, filtered, and evaporated. The product was purified by centrifugal chromatography on silica gel with 9:1 hexanes to methylene chloride as eluent to yield ~15 mg (20%) of a pale yellow solid. Mp: 118−121 °C. ^{1}H NMR (500 MHz, $CDCl_3$): δ 3.85 (d, J = 13 Hz, 2H), 5.09 (d, J = 13.5 Hz, 2H), 7.63 (s, 2H), 7.74 (d, J = 9 Hz, 2H), 7.79 (s, 2H), 7.82 (d, J = 8 Hz, 2H). ^{13}C NMR (125 MHz, $CDCl_3$): δ 24.0, 123.1, 126.96, 126.99, 127.8, 128.67, 130.4, 130.7, 135.4, 136.2, 136.3, 137.0. HRMS: found, 356.0091; calcd ($C_{22}H_{12}$Se), 356.0104. UV−vis (CH_2Cl_2) [λ_{max} (ϵ)]: 227 (3800), 256 (4200), 293 (2200).

2,3-Dihydro-1*H*-corannuleno[2,3-*cd*]thiopyran (7). To a 25 mL round-bottom flask equipped with a reflux condenser were added 2,3-bis(bromomethyl)corannulene (**3b**) (0.050 g, 0.115 mmol) and acetone (10 mL). Sodium sulfide nonahydrate (0.041 g, 0.173 mmol) was added as a solution in DMSO (5 mL) (reaction turns dark black) and the solution heated to 80 °C for 10 min. The reaction was quenched with water, diluted with methylene chloride (25 mL), and extracted three times with water (100 mL). The organic layer was dried with magnesium sulfate, filtered, and evaporated. The product was purified by centrifugal chromatography on silica gel with 2:1 hexanes to methylene chloride as eluent to yield ~25 mg (35%) of a pale yellow solid. Mp: 125−128 °C. ^{1}H NMR (500 MHz, $CDCl_3$): δ 3.83 (d, J = 14.5 Hz, 2H), 4.90 (d, J = 14.5 Hz, 2H), 7.57 (s, 2H), 7.75 (d, J = 9 Hz, 2H), 7.78 (s, 2H), 7.82 (d, J = 8.5 Hz, 2H). ^{13}C NMR (100 MHz, $CDCl_3$): δ 33.1, 123.1, 126.7, 126.9, 127.5, 127.8, 130.50, 130.54, 135.4, 135.6, 135.9, 136.2. HRMS: found, 308.0653; calcd ($C_{22}H_{12}S$), 308.0660. UV−vis (CH_2Cl_2) [λ_{max} (ϵ)]: 227 (3900), 256 (4400), 293 (2100).

2,3-Dihydro-2′,2′ -bis(carboxyethyl)-1*H*-corannuleno[2,3-*cd*]benzene (8a). In a 50 mL round-bottom flask equipped with a reflux condenser, sodium (0.010 g, 0.435 mmol) was added to ethanol (25 mL) and allowed to stir at ambient temperature until all the metal was consumed. The solution was cooled on an ice bath for 10 min. A solution of 2,3-bis(bromomethyl)corannulene (**3b**) (0.075 g, 0.172 mmol) and diethyl malonate (0.028 g, 0.172 mmol) in tetrahydrofuran (5 mL) and ethanol (5 mL) was added to the sodium ethoxide solution. The solution was stirred at ambient temperature for 12 h. The reaction was quenched with water, diluted with ether (25 mL), and extracted three times with water (100 mL). The organic layer was dried with magnesium sulfate, filtered, and evaporated. The product was purified by centrifugal chromatography on silica gel with 6:4 hexanes to methylene chloride as eluent to yield ~15 mg (15%) of a pale yellow solid. Mp: 98−100 °C. ^{1}H NMR (400 MHz, $C_2D_2Cl_4$ at 10 °C): δ 0.87 (t, J = 6.8 Hz, 3H), 1.26 (t, J = 7.2 Hz, 3H), 3.56 (d, J = 15.6 Hz, 2H), 3.70 (q, J = 6.8 Hz, 2H), 3.96 (d, J = 15.6 Hz, 2H), 4.25 (q, J = 6.8 Hz, 2H), 7.50 (s, 2H), 7.72 (d, J = 8.4 Hz, 2H), 7.76 (s, 2H), 7.77 (d, J = 8.8 Hz, 2H). ^{13}C NMR (100 MHz, $C_2D_2Cl_4$ at −10 °C): δ 14.0, 14.4, 36.1, 57.8, 61.9, 62.6, 124.1, 127.3, 127.7, 127.8, 128.6, 130.8, 132.4, 135.4, 135.57, 135.65, 136.8, 170.4, 171.3. HRMS: found, 434.1521; calcd ($C_{29}H_{22}O_4$), 434.1518. UV−vis (CH_2Cl_2) [λ_{max} (ϵ)]: 255 (3700), 292 (2000), 341 (360).

2,3-Dihydro-*N*-phenyl-1*H*-corannuleno[2,3-*cd*]pyridine (9a). To a 50 mL round-bottom flask equipped with a reflux condenser were edded 2,3-bis(bromomethyl)corannulene(**3b**) (0.044 g, 0.100 mmol) and dry 1,2-dimethoxyethane (25 mL) under a stream of argon. Aniline (0.093 g, 0.100 mmol) was added to the solution followed by sodium hydride (0.012 g, 0.300 mmol, 60% dispersion in oil), and the solution was heated to reflux for 12 h. The reaction was quenched with water and extracted 3 times with water (100 mL). The organic layer was dried with magnesium sulfate, filtered, and evaporated. The product was purified by centrifugal chromatography on silica gel with 1:1 hexanes to benzene as eluent to yield ~13 mg (35%) of a pale yellow solid. Mp: 186−188 °C. ^{1}H NMR (500 MHz, $C_2D_2Cl_4$): δ 4.52 (d, J = 15.5 Hz, 2H), 5.12 (d, J = 16 Hz, 2H), 6.81 (t, J = 7.5 Hz, 1H), 7.09 (d, J = 7.5 Hz, 2H), 7.22 (d, J = 8 Hz, 2H), 7.53 (s, 2H), 7.73 (d, J = 8.5 Hz, 2H), 7.74 (s, 2H), 7.76 (d, J = 8.5 Hz, 2H). ^{13}C NMR (75 MHz, $CDCl_3$): δ 50.1, 114.3, 117.0, 118.3, 118.4, 123.7, 124.1, 124.3, 125.8, 126.1, 127.4, 129.2, 132.5, 132.8, 133.3, 147.2. HRMS: found, 367.1369; calcd ($C_{28}H_{17}N$), 367.1361. UV−vis (CH_2Cl_2) [λ_{max} (ϵ)]: 228 (4800), 257 (4400), 290 (3000), 340 (330).

2,3-Dihydro-1*H*-corannuleno[2,3-*cd*]pyran (10). To a 50 mL round-bottom flask equipped with a reflux condenser were added 2,3-bis(bromomethyl)corannulene (**3b**) (0.050 g, 0.115 mmol) and 1,2-dimethoxyethane (25 mL). Potassium hydroxide (1 mL, 10% in water) was added, and the solution was heated to reflux for 4 h. The reaction was cooled and allowed to stir at ambient temperature for 12 h. The reaction was quenched with water, diluted with methylene chloride (25 mL), and extracted 3 times with water (100 mL). The organic layer was dried with magnesium sulfate, filtered, and evaporated. The product was purified by centrifugal chromatography on silica gel with 1:1 hexanes to methylene chloride as eluent to yield ~20 mg (50%) of a pale yellow solid. Mp: 218−220 °C. ^{1}H NMR (400 MHz, $CDCl_3$): δ 4.76 (d, J = 14.8 Hz, 2H), 5.49 (d, J = 14.8 Hz, 2H), 7.42 (t, J = 1.2 Hz, 2H), 7.74 (d, J = 8.8 Hz, 2H), 7.76 (s, 2H), 7.78 (d, J = 8.8 Hz, 2H). ^{13}C NMR (100 MHz, $CDCl_3$): δ 69.3, 119.6, 126.7, 127.2, 127.3, 127.7, 130.5, 132.4, 135.9, 136.2, 136.3, 136.5. HRMS: found, 292.0887; calcd ($C_{22}H_{12}O$), 292.0888. UV−vis (CH_2Cl_2) [λ_{max} (ϵ)]: 226 (3800), 256 (4400), 291 (3000), 340 (380).

2,3-Diphenylcorannulene (4). To 50 mL round-bottom flask equipped with a reflux condenser were added 2,3-dichlorocorannulene (**2a**) (0.050 g, 0.157 mmol) and dry, distilled tetrahydrofuran (25 mL) under a stream of argon. (1,3-Bis(diphenylphosphino)propane)nickel-(II) chloride (0.009 g, 0.016 mmol) was added followed by slow addition of phenylmagnesium bromide (1.57 mL, 1.57 mmol, 1.0 M in tetrahydrofuran). The solution was refluxed for 4 h and then cooled to ambient temperature. The reaction was quenched by slow addition

of water, diluted with methylene chloride (25 mL), and extracted 3 times with water (25 mL). The organic layer was dried over magnesium sulfate, filtered, and evaporated. The product was purified by column chromatography on silica gel with 9:1 hexane to benzene as eluent to yield 25 mg (40%) of a white solid. Mp: 210−212 °C. ^{1}H NMR (500 MHz, CD_2Cl_2): δ 6.97 (td, ^3J = 8.5 Hz, ^4J = 1.5 Hz, 4H), 7.02 (tt, ^3J = 7.5 Hz, ^4J = 1.5 Hz, 2H), 7.10 (dd, ^3J = 7.5 Hz, ^4J = 2 Hz, 4H), 7.75 (s, 2H), 7.87 (d, J = 8.5 Hz, 2H), 7.90 (s, 2H), 7.92 (d, J = 8.5 Hz, 2H). ^{13}C NMR (100 MHz, CD_2Cl_2): δ 126.4, 127.0, 127.29, 127.34, 127.5, 127.7, 129.4, 130.0, 130.3, 131.0, 134.8, 135.6, 135.9, 141.8, 142.9. HRMS: found, 402.1396; calcd ($C_{34}H_{18}$), 402.1409. UV−vis (CH_2Cl_2) [λ_{max} (ϵ)]: 253 (5400), 288 (4000), 342 (240).

2,3-Bis(2-(2-methoxyethoxy)ethoxy)corannulene (5). To a 25 mL round-bottom flask equipped with a reflux condenser were added sodium hydride (0.200 g, 8.33 mmol) and diethylene glycol monomethyl ether (25 mL). 2,3-Dichlorocorannulene (**2a**) (0.032 g, 0.100 mmol) was added, and the solution was heated to 170 °C for 12 h and then cooled to ambient temperature. The solvent was evaporated, and the product was purified by column chromatography on silica gel with 98:2 methylene chloride to methanol as eluent to yield ∼15 mg (25%) of a clear oil. ^{1}H NMR (500 MHz, CD_2Cl_2): δ 3.36 (s, 6H), 3.58 (t, J = 5 Hz, 4H), 3.76 (t, J = 4 Hz, 4H), 3.99 (t, J = 4.5 Hz, 4H), 4.38 (t, J = 4.5 Hz, 4H), 7.08 (s, 2H), 7.71 (d, J = 8.5 Hz, 2H), 7.76 (s, 2H), 7.81 (d, J = 9 Hz, 2H). ^{13}C NMR (100 MHz, $CDCl_3$): δ 59.1, 69.6, 69.8, 70.8, 72.1, 94.3, 105.7, 117.2, 125.8, 126.1, 127.7, 129.4, 130.3, 132.6, 136.0, 157.6. HRMS: found, 486.2023; calcd ($C_{30}H_{30}O_6$), 486.2042.

2,7-Bis(bromomethyl)-4,5-dichlororcorannulene (2c). In a 50 mL round-bottom flask equipped with a reflux condenser, 1,6-dimethyl-3,4-dichlorocorannulene (**2b**) (0.032 g, 0.093 mmol) was added to carbon tetrachloride (25 mL) under argon. With an incandescent light shining on the solution, benzoyl peroxide (∼2 mg) followed by *N*-bromosuccinimide (0.033 g, 0.186 mmol) was added. The solution was stirred at ambient temperature. After 3 h a precipitate formed and the solvent was evaporated to a yellow solid. Trituration twice with methanol (10 mL) yielded 50 mg (quantitative) of a pale yellow solid. Mp: >300 °C. ^{1}H NMR (400 MHz, CD_2Cl_2): δ 5.02 (s, 2H), 7.82 (s, 2H), 7.89 (s, 2H), 8.18 (s, 2H). ^{13}C NMR: solubility too poor for measurement. HRMS: found, 501.8523; calcd ($C_{22}H_{10}Br_2Cl_2$), 501.8526.

2,7-Bis(methoxymethyl)-4,5-dichlororcorannulene (2d). In a 50 mL round-bottom flask equipped with a reflux condenser, 2,7-bis-(bromomethyl)-4,5-dichlorocorannulene (**2c**) (0.019 g, 0.038 mmol) was added to a solution of sodium methoxide (0.020 g, 0.376 mmol) in methanol (25 mL) and tetrahydrofuran (10 mL). The solution was heated to reflux for 2 h and cooled to ambient temperature. The reaction was quenched with water, diluted with methylene chloride (25 mL), and extracted three times with water (25 mL). The organic layer was dried over magnesium sulfate, filtered and evaporated to yield 15 mg (90%) of a pale yellow solid. Mp: 185−187 °C. ^{1}H NMR (500 MHz, CD_2Cl_2): δ 3.49 (s, 6H), 4.91 (s, 4H), 7.81 (s, 4H), 8.12 (s, 2H). ^{13}C NMR (125 MHz, CD_2Cl_2): δ 58.3, 72.8, 124.0, 127.31, 127.32, 127.4, 130.1, 130.5, 130.8, 133.9, 135.1, 135.5, 135.9. HRMS: found, 406.0522; calcd ($C_{24}H_{16}Cl_2O_2$), 406.0527. UV−vis (CH_2Cl_2) [λ_{max} (ϵ)]: 229 (5400), 262 (5700), 295 (5000), 341 (380).

2,5-Bis(bromomethyl)corannulene (12b). To a 250 mL round-bottom flask equipped with a reflux condenser were added 2,5-dimethylcorannulene (**12a**) (0.123 g, 0.441 mmol) and carbon tetrachloride (100 mL) under a stream of argon. *N*-Bromosuccinimide (0.157 g, 0.883 mmol) was added to the solution followed by benzoyl peroxide (∼5 mg). The solution was irradiated with an incandescent light for 4 h at room temperature. The reaction was quenched with water and extracted 3 times with water (100 mL). The organic layer was dried with magnesium sulfate, filtered, and evaporated. The solid was triturated twice with methanol (10 mL) to yield 0.175 g (90%) of a pale yellow solid. ^{1}H NMR (500 MHz, $CDCl_3$): δ 5.07 (s, 4H), 7.75 (d, J = 8.7 Hz, 2H), 7.79 (d, J = 8.7 Hz, 2H), 7.84 (s, 2H), 7.83), 8.14 (s, 2H).

1,6-Bis(bromomethyl)corannulene (13b). To a 50 mL round-bottom flask equipped with a reflux condenser were added 1,6-dimethylcorannulene (**13a**) (0.320 g, 1.15 mmol) and carbon tetrachloride (30 mL) under a stream of argon. *N*-Bromosuccinimide (0.420 g, 2.36 mmol) was added to the solution followed by benzoyl peroxide (∼5 mg). The solution was irradiated with an incandescent light for 4 h at room temperature. The reaction was quenched with water and extracted 3 times with water (100 mL). The organic layer was dried with magnesium sulfate, filtered, and evaporated. The solid was triturated twice with methanol (10 mL) to yield 0.450 g (90%) of a pale yellow solid. Mp: 255−258 °C (dec). ^{1}H NMR (300 MHz, $CDCl_3$): δ 5.04 (s, 4H), 7.74 (s, 2H), 7.80 (s, 2H), 7.89 (d, J = 8.7 Hz, 2H), 8.06 (d, J = 9.0 Hz, 2H). ^{13}C NMR (125 MHz, $CDCl_3$): δ 31.3, 125.3, 127.6, 127.8, 128.3, 129.6, 131.0, 131.1, 135.7, 136.0, 136.6, 136.7. HRMS: found, 433.9320; calcd ($C_{22}H_{12}Br_2$), 433.9306.

(Bromomethyl)corannulene (14b). To a 50 mL round-bottom flask equipped with a reflux condenser were added methylcorannulene (**14a**) (0.035 g, 0.13 mmol) and benzene (20 mL) under a stream of argon. *N*-Bromosuccinimide (0.024 g, 0.13 mmol) was added to the solution followed by benzoyl peroxide (∼5 mg). The solution was irradiated with an incandescent light for 4 h at room temperature. The reaction was quenched with water and extracted 3 times with water (20 mL). The organic layer was dried with magnesium sulfate, filtered, and evaporated. The solid was triturated twice with methanol (10 mL) to yield 0.040 g (90%) of a pale yellow solid. ^{1}H NMR (500 MHz, $CDCl_3$): δ 5.07 (s, 2H), 7.76 (d, J = 9.0 Hz, 1H), 7.80 (m, 7H), 8.06 (d, J = 9.0 Hz, 1H). ^{13}C NMR (125 MHz, $CDCl_3$): δ 31.2, 124.6, 126.9, 127.1$_0$, 127.1$_4$, 127.2, 127.4$_8$, 127.5$_0$, 127.9, 130.4, 130.5, 130.9, 131.0$_0$, 131.0$_1$, 131.2, 135.7$_0$, 135.7$_3$, 135.8, 136.0, 136.1$_6$, 136.1$_8$. HRMS: found, 342.0029; calcd ($C_{21}H_{11}Br$), 342.0044.

Acknowledgment. This work was supported by the National Science Foundation (Grant CHE-9904275) and the National Institute of Heath (Grant NIH P41 RR08605-06). Supercomputer time was provided by a grant from the SDSC National Resource Allocation Program. This work was also supported by a stipend of the German Academic Exchange Service (DAAD) for G.H.G.

Supporting Information Available: Variable-temperature ^{1}H NMR spectra and tables of computational data for all pertinent compounds. This information is available free of charge via the Internet at http://pubs.acs.org.

JA0019981